Innovative Composite Deck Slab for Railway Bridges. Finite Element Studies and Comparison with Test Results

Paul Herrmann[1] *& Josef Fink*[2]

Keywords: sandwich structure; steel-concrete composite; shear connectors; finite element method; parametric studies

Abstracts: The Institute of Steel Structures on Vienna University of Technology is developing a new, extremely slender steel-concrete-steel composite (SCSC) plate which is intended to be used in the substitution of old railway bridges without ballast bed. The plate consists of an unreinforced concrete core sandwiched by two steel plates. Dowel strips, welded alternately to the outer steel plates, work together with the concrete core as shear force connection elements. The static strength of the slab was experimentally investigated in full scale laboratory tests. The next step for a derivation of mathematical models is the FE modelling and analysis including highly sophisticated nonlinear material models. Some of the required material variables cannot be identified by physical strength tests. Therefore, parametric studies and the assessment of the influence of each parameter are necessary to find the "best fitting" parameter combinations.

1. Introduction

1.1 Motivation

A fair amount of old railway bridges is reaching the end of its technical life cycle. Therefore, these bridges need to refurbished or replaced by new structures. At the time of their design the open railway deck, where the sleepers are mounted directly on the steel superstructure, was considered as state of the art. This type of railway deck is characterised by an extremely low construction depth between the bottom edge of the construction (BE-C in Fig. 1) and the top of the sleepers (TE-S in Fig. 1).

1 Vienna University of Technology, Karlsplatz 13, A-1040 Vienna, Austria, paul.herrmann@tuwien.ac.at
2 Univ.Prof. Dipl.Ing. Dr.techn., Vienna University of Technology, Karlsplatz 13, Austria – 1040 Vienna, josef.fink@tuwien.ac.at

E. Petzek, R. Băncilă (Eds.), *The Eight International Conference "Bridges in Danube Basin",*
DOI 10.1007/978-3-658-03714-7_16,

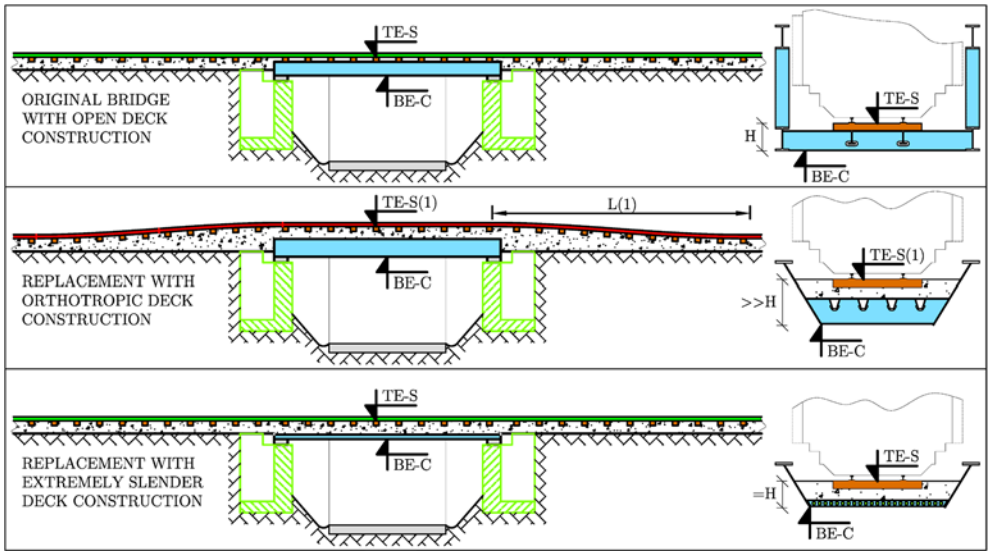

Figure 1: Motivation for the development of extremely slender deck constructions

On one hand, the open deck cannot be used any more for modern railway bridges for reasons of its high noise emission. On the other hand, it is usually impossible to change the levels of the clearance under and of the rail track on the bridge.
This often results in the discrepancy between the low given construction depth and the relatively high demand of modern railway track systems like the ballast bed or the nonballasted track. Fig. 1 shows the described problem in a schematic view.

This specific problem can only be solved by the use of extremely slender deck slab constructions. The Institute of Structural Engineering/ Steel Structures is therefore developing a trough bridge system for the Austrian railways, which is applicable for spans up to 25m and shall meet the objectives described above.

This bridge system contains conventional top flanges and webs while the track slab is a new, innovative and extremely slender steel-concrete-steel composite (SCSC) plate (Fig. 2).

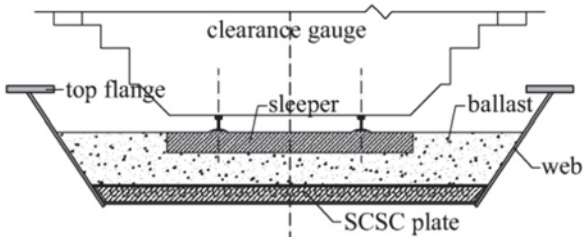

Figure 2: Trough bridge with SCSC plate [Fink et al. 2010]

1.2 Basic description of the SCSC-Plate

The SCSC-plate provides an excellent load bearing capacity at an extremely low construction height. The main idea is to generate the necessary bending moment resistance by steel layers which are placed at the highly stressed outer zones of the cross section while a more economical material like concrete is used in the zones near to the neutral axis. A shear force resistant connection of the outer steel parts is necessary to activate their "Steiner"-parts. Furthermore the outer steel plates work as a sealing of the whole concrete surface and therefore increase the durability in comparison to conventional reinforced concrete decks.

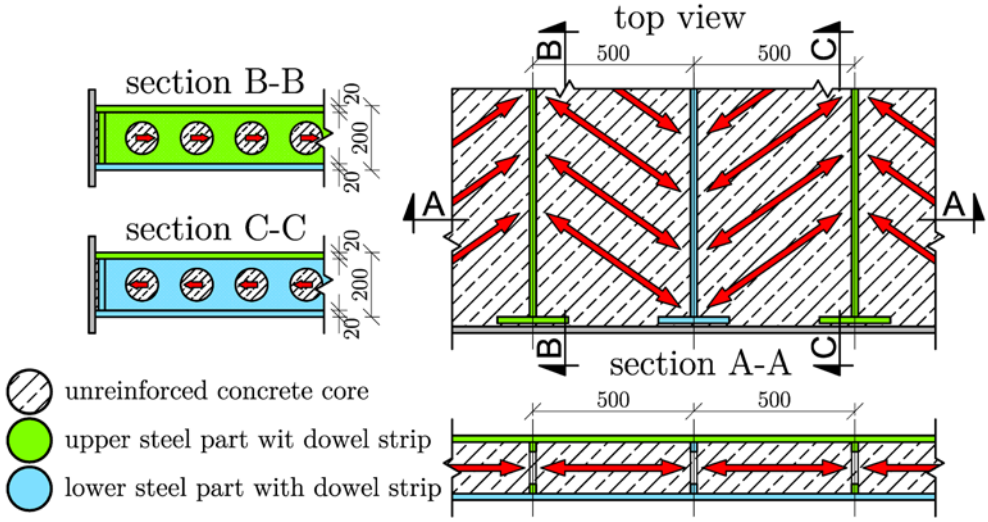

Figure 3: Basic construction and load bearing mechanism- dowel type C (unit: mm)

The two outer steel plates are interconnected by dowel strips, which are welded alternately to the upper and the lower side and work together with the concrete core as the required shear connection elements. The basic idea to ensure the shear force transmission between the upper (green in Fig. 3) and the lower (blue in Fig. 3) steel part is the formation of compression diagonals within the concrete core (indicated by red arrows in Fig. 3). Thereby the horizontal portion of each diagonal member is in equilibrium with horizontal portion of a diagonal member in the adjacent chamber and a reinforcement of the filling concrete is obsolete.

1.3 Laboratory tests

In the course of the investigations the flexural and shear behaviour of the slab construction was experimentally tested in the laboratory of the Institute of Structural Engineering (see [Fink et al. 2010], [Juen & Fink 2011], [Fink & Juen 2010], [Fink et al. 2011]). A total number of four SCSC plate specimens (Type A – Type D) were tested at a span of 2520 mm, subjected to a static linear load along one centred application line below the specimens. Due to the test setup the specimens were bent upwards. The overall maximum test load for specimen type "A" was limited to about 6650kN.

Overall, 37 strain gauges (SGs) and 10 linear variable displacement transducers (DTs) were applied to each specimen. The test data, which was obtained from the laboratory tests, will further be used to evaluate and validate the results of the various finite element models.

2. Finite Element Modelling

A knowledge of effects which are not measurable during laboratory tests can be very helpful for the derivation of further engineering models. Especially the multiaxial strain distribution in the unreinforced concrete at different load stages can only be investigated by the help of finite element (FE-) simulations. Therefore the laboratory test procedures were numerically simulated with the FE- package [Abaqus 2010a].

2.1 General requirements

2.1.1 Integration method and element types

The FE method basically provides two different methods for the incremental integration of nonlinear problems. These methods are the implicit and the explicit integration algorithm. The implicit integration is based on equilibrium considerations on each incremental step. Starting from the time point "t" the incremental step "t+Δt" is determined with an actual "tangent stiffness". After that the difference of inner and outer forces is minimized by an incremental iteration of deformations and subsequent equilibrium calculations. The implicit integration algorithm can lead to divergence effects at decreasing load- deflection paths after yielding or passing the ultimate load resistance. Therefore this algorithm is not applicable for investigations of load- controlled laboratory tests.

The explicit integration is a dynamic calculation method, based on the incremental solution of the kinetic equilibrium in each time step. The partial differential equation of motion is solved by the help of the central difference operator. The explicit integration method does not require subsequent equilibrium iterations, which can increase the calculation time significantly. Even though the time increments "Δt" in explicit calculations are usually smaller than in implicit iterations, the numerical cost is typically less. FE- simulations which shall pass yielding effects or ultimate load points can be described by explicit integration methods. Static load scenarios can be assessed in a quasi-static way by reducing the damping- and mass inertia forces to negligible values with a sufficiently slow "loading velocity" [Zimmermann 2001]. ABAQUS offers the explicit integration algorithm DYNAMIC EXPLICIT, which was used for all analysis [Abaqus 2010b].

The complex structure of the SCSC-plate can only be described by the use of three-dimensional volume elements. ABAQUS offers linear tetrahedral or hexahedral elements for the use within DYNAMIC EXPLICIT. Tetrahedral elements usually reproduce the structural behaviour too stiff and therefore need an extremely fine mesh for accurate results. Linear hexahedral elements can show the effect of "shear- locking", which also results in an unrealistic assumption of the stiffness. Linear hexahedral elements with reduced integration do not show this effect. Besides of that, these elements need significantly less numerical cost during the integration process. The known problem of "hourglassing" can be minimized by the use of a relatively fine mesh, precisely by the use of two or more element layers per steel

plate. Hence the investigated FE models were all meshed by C3D8R element, which are linear hexahedral elements with reduced integration.

1.1.1. Materials- constitutive models

The numerical FE calculations shall simulate the laboratory tests up to the load of plastic failure. Hence it is necessary to use nonlinear material models for both, the steel and the concrete parts.

ABAQUS contains the material model CLASSIC METAL PLASTICITY (CMP), which describes the nonlinear behaviour of steel, based on the calculation of the equivalent von Mises stresses and the full stress- strain curve. The values of yield- and tensile strength and of the elongation after fracture are taken from the original inspection certificates of the used steel plates.

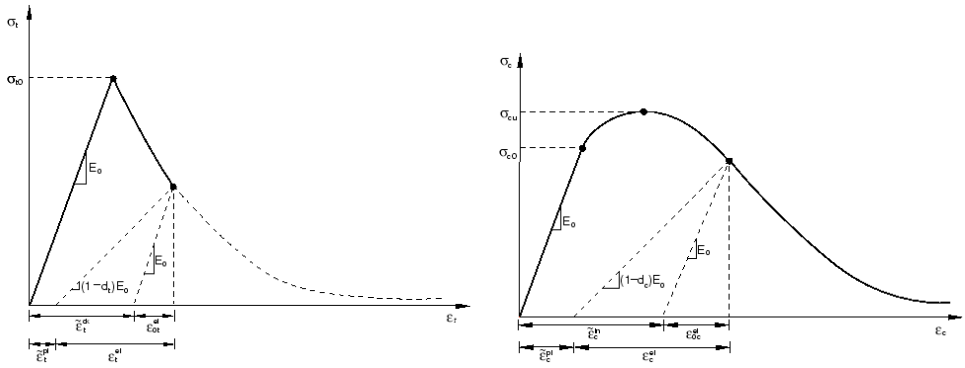

Figure 4: Stiffness decrease of the material Model CDP for tension (left) and compression (right) stresses [Abaqus 2010b]

A proper description of the concrete parts is more complex and requires highly sophisticated material models. ABQUS therefore offers a big number of possibilities. Here, only the used model CONCRETE DAMAGED PLASTICITY (CDP), an anisotropic nonlinear material model which considers a strain dependent decrease of stiffness for both, compression and tension stresses, will be presented. The uniaxial stress- strain curves can be described in accordance with laboratory test data of compression strength tests. The consideration of the stiffness decrease of damaged concrete is modelled in CDP by the implementation of the tension damage parameter d_t and the compression damage parameter d_c, which reduce the effective Young's modulus for inelastic stress levels. Fig. 4 shows the application of these damage parameters.

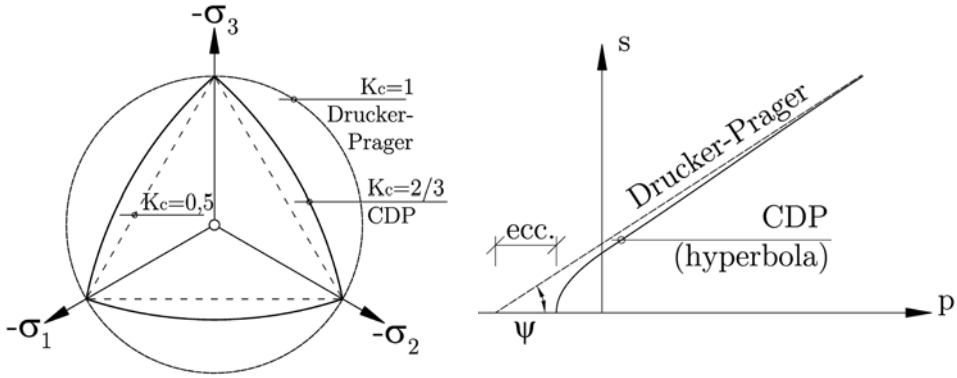

Figure 5: Modification in deviatoric cross section (left) and in meridional plane (right)

The plastic boundary surface of CDP was first presented in [Lubliner et al. 1989] and later refined in [Lee & Fenves 1998]. It is based on the classical Drucker- Prager model and contains three modifications.

The modification in the deviatoric cross section is shown in Fig. 5 on the left. It defines a geometrical deviation from the known circle of the Drucker- Prager model and can be described by the parameter Kc. The value of Kc needs to be chosen between 0,5 and 1,0. The default value, which is recommended in [Lubliner et al. 1989] is 0,67.

The second modification can be seen in the meridional plane on the right of Fig. 5. It defines the generating function of the plastic boundary surface as a hyperbola, which can be described by two variables. The eccentricity (ecc.) describes the rate of approach to the asymptotes which are actually the generating lines of the classical Drucker- Prager criterion. [Lubliner et al. 1989] recommends an eccentricity value of 0,1. The second variable, the dilation angle ψ, describes the inclination of the asymptotes. It can be understood as the angle of inner friction of the material is and therefore limited to 45°. In the literature the suggested values of ψ vary from 12° to 45° [Fink et al. 2007].

The third modification limits the maximum compression resistance for multiaxial stress states. The value which defines this limitation is the ration of the biaxial and the uniaxial compression resistance. This ratio is recommended to be set to 1,16. [Abaqus 2010b] particularly points out, that the model CDP is not applicable for high hydrostatical compression states. It is advised not to use the results of this material model in areas of multiaxial compression with stresses, which are exceeding approximately five times the uniaxial resistance.

2.1.2 FE- model generation

In the following, the geometry of the used FE model shall be described roughly. The high number of elements combined with nonlinear material and contact formulations as well as the application of the theory of large deformations cause a huge numerical cost. Therefore it is necessary to seize all given symmetries and thus reduce the calculation time as much as possible. Fig. 6 shows the resulting plate section, using symmetry in x- and y- direction.

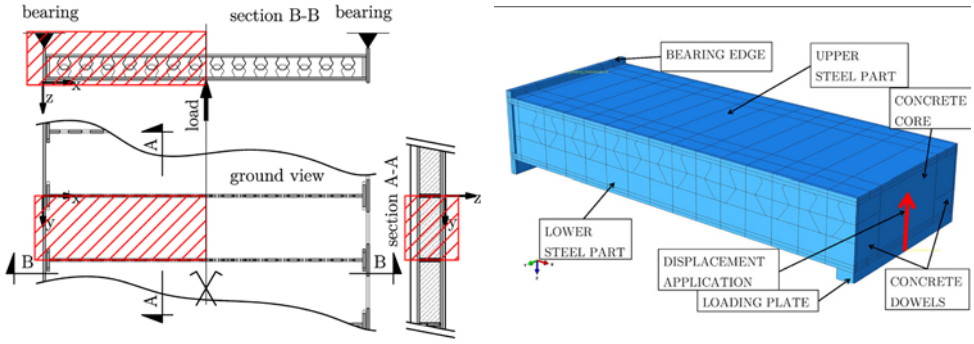

Figure 6: Analysed plate section (left) and assembly of the FE- model (right)

The numerical FE- model is divided into several parts which are assembled together after creation. The main parts are the upper and the lower steel part, the concrete core, the concrete dowels and the load application plate. The figure shows the finished assembly on the right. The "bearing edge" is supported in z direction while out of plane deformations are blocked on all symmetry planes. The model is loaded by a displacement of the "loading plate". This displacement is displayed as a red arrow.

For more detailed information about the creation of parts, the interaction properties, the assembly and load application, see [Herrmann 2013].

2.2 Identification of variation parameters

Due to the explanations above, all investigations are done with the explicit integration algorithm and the material models CMP and CDP in combination with C3D8R elements. These fixed parameters already were identified as the best option in former research work of the institute [Fink et al. 2007]. The mesh of the base model is refined in accordance with the guidelines of [Abaqus 2010b] until obvious hourglass effects disappear and the calculation process is sufficiently stable. During the parametric studies, the influence of the mesh resolution is not investigated particularly.

As mentioned above, four different plate specimens with varying shapes of the used dowel strips were tested experimentally in the laboratory. The FE- analysis in [Herrmann 2013] is just done for two specimen geometries, more precisely Type A and Type C. This paper just refers to the analysis of plate specimen Type A, which contains the Vienna Crown Dowel geometry. The plate type is indicated by the letter "A" in the model name in Fig.7.

A	1ms	CDP2	f70	Psi45	DP55
specimen type	loading velocity	tension damage parameter	friction coeff.	dilation angle	compression damage parameter

Figure 7: Name scheme to label the parameter combination of an FE- model

The influence of the loading velocity was identified as minor in former works [Antesberger 2007]. Therefore the major part of the investigated FE- models is calculated with a loading velocity of 1,0mm/sec (1ms in the model name in Fig. 7). The low influence of a differing velocity is verified afterwards by the investigation of some models, loaded with 0,5mm/sec (05ms in the model name).

The influence of the dilation angle y is predicted to be high and therefore varied in a relatively wide range. More precisely the investigated values are 30°, 40° and the absolute maximum of 45°. The dilation angle of the actual model is indicated by Psi30, Psi40 or Psi45 in the model name in Fig. 7.

Former scientific FE- analysis of laboratory tests identified the friction coefficient as a leading variation parameter ([Fink et al. 2006], [Antesberger 2007]). Since it is impossible to ensure or predict sufficiently constant friction conditions in most of the contact joints of the SCSC-plate specimen, nearly all of these joints are regarded as frictionless within the calculation. This leads to a secure estimation and slightly lower bearing capacities in the calculation models. Friction is only considered in the highly stressed joints on the flame cut steel dowel front faces. In these areas the friction coefficients are set to 30%, 50% or 70% (f30, f50 or f70 in the model name in Fig. 7).

The definition of the damage parameters depends of strains or crack displacements and can therefore not be expressed in single values. The characteristics of the tension damage parameter d_t are taken from an exemplary model of a concrete gravity dam in the ABAQUS Example Problems Manual [Abaqus 2010b] and are indicated by the label CDP1 in the model name in Fig. 7. Within the mentioned example, CDP is used to describe a reinforced concrete structure and therefore considers a relatively high tension stress resistance after cracking while the resistance of the unreinforced concrete core of the test specimens is possibly very low. Therefore the tension damage behaviour is investigated in a second set of parameters by taking into account the same damage gradient at only 50% of the crack displacement values (CDP2 in the model name in Fig. 7). This is a numerically stable possibility to simulate a tension resistance close to zero after exceeding the tensile strength of concrete. Fig. 8 shows the stress- crack displacement and the stress- damage variable relations of the two investigated alternatives.

The influence of the maximum compression damage parameter d_c is investigated in two steps. First, the parametric studies are done with a maximum compression damage parameter of 0,55, indicated by the label DP55 in the model name in Fig. 7. Afterwards, the best fitting model is alternatively analysed with a maximum compression damage parameter of 0,20 (DP20 in the model name) and finally without any stiffness decrease (DP00 in the model

name). Fig. 9 shows the stress- strain curve as well as the relation between the inelastic strain and the damage variable relations of the three investigated alternatives.

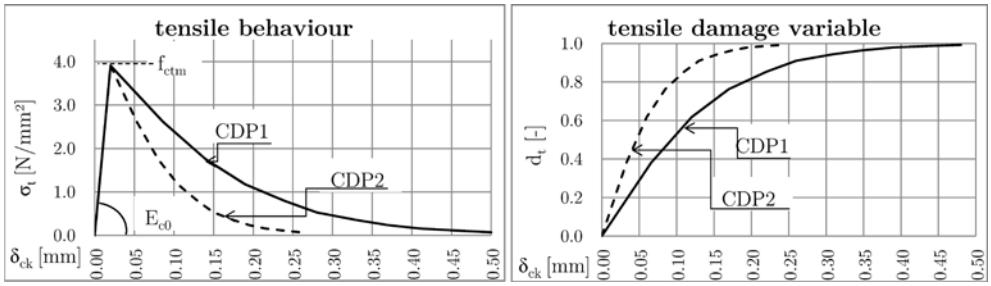

Figure 8: Variation of tensile behaviour (left) tensile damage (right) in the parametric studies

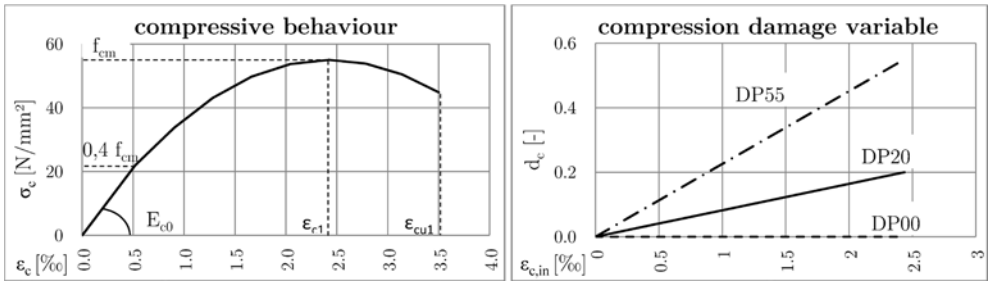

Figure 9: Variation of compressive behaviour (left) compression damage (right) in the parametric studies

3. Results of the parametric studies

3.1 Influence of variation parameters

As a first step to find out the best fitting combination of parameters, the obtained results of the FE- simulations are compared to the experimentally determined data of the laboratory tests. The following chapters will only present comparisons of midspan deflections.

3.1.1 Dilation angle, friction coefficient and tension damage parameter

The influences of the variation parameters “dilation angle” and “friction coefficient” will be presented as a unity. Black letters in the model names in Fig. 10 and 11 mean fixed parameters while coloured letters indicate the variation set.

Fig. 10 already allows two basic interpretations which are not varying significantly within the entire parametric studies. The first common effect is that the linear elastic range of the force- deflection curves of any FE- model is in fair accordance with the measured displacements of the laboratory tests. This range can be specified up to a midspan deflection

of about 10mm and a total vertical load of approximately 3000kN. The second conclusion is that it is not possible to describe the structural behaviour of decreasing load resistance beyond the maximum plastic load with any FE- model. Hence the numerical results above a central deflection of roughly 45mm respectively a total load of about 6000kN should not be used for interpretation.

The dilation angle of y=30° causes a sharp bend of the curves at a deflection level of about 20mm and therefore an unrealistically low plastic resistance while an angle of 45° allows a better approximation of the measured deformation. The friction coefficient does obviously not influence the results in a significant way but can be varied to stabilise the calculation process. However it is impossible to point out a recommendation for one specific friction coefficient. Depending on the parameter combination, different coefficients result in the smoothest curves.

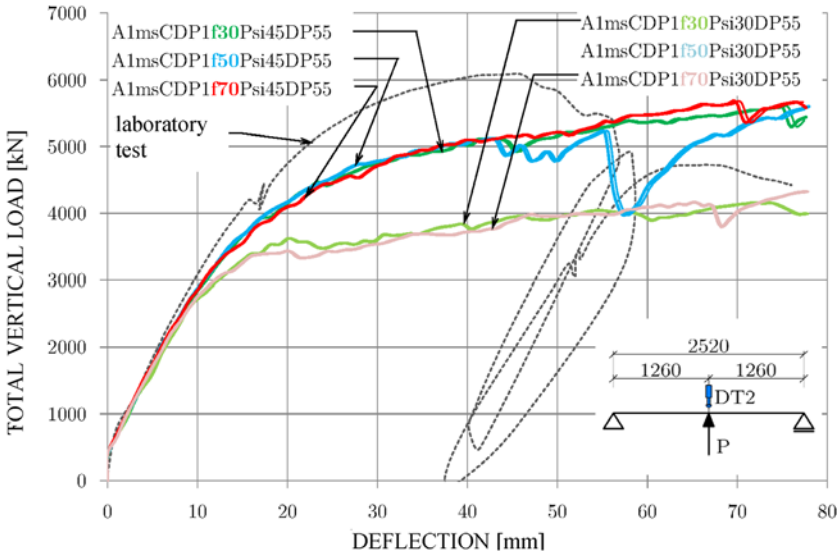

Figure 10: Variation of friction and dilation angle on A1msCDP1 and DP55

Fig. 11 shows the load- deflection curves of the two “best fitting” models of Fig. 10 (A1ms-f30Psi45DP55 and A1ms-f70Psi45DP55) with increased tension damage (CDP2). The friction coefficient of 70%, which results in the best approximation with CDP1 (see Fig.10), causes numerical instabilities in combination with CDP2. Obviously, the models of CDP2 result in slightly lower load resistance. However, the difference is not significantly high and the application of CDP2 is theoretically more consistent. Therefore it is recommended to use the material formulation of increased tension damage (CDP2).

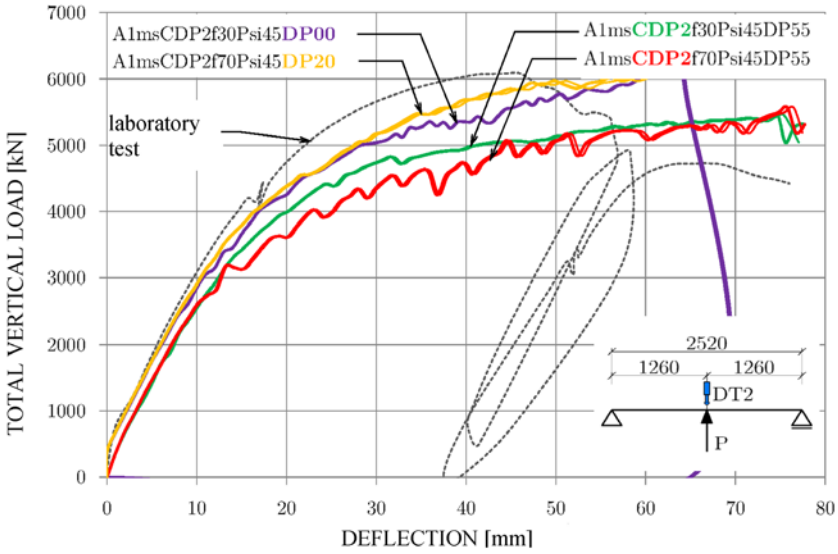

Figure 11: Influence of damage parameter on A1msCDP2f30(70)Psi45 – deflections

3.1.2 Compression damage parameter

The concrete core in the SCSC-plate is enclosed in a steel box and can therefore not collapse in the same way like concrete parts with free surfaces. Hence it is understandable that this special case is described in a better way with concrete models of poor compression damage rates. The variation of d_c in Fig. 11 approves the vast influence of the compression damage parameter. The measured load- deflection behaviour of the laboratory tests can be approached best by the model A1msCDP2f70Psi45DP20. Especially the plastic deformations at midspan deflections between 10mm and 45mm can be described with a smooth curve in a satisfying way. A concrete modelling without any compression damage (DP00) shows a worse approximation. A1msCDP2f70Psi45DP20 also results in a significantly better accuracy of the load- strain curves of all strain gauges, which cannot be shown here. For further information and diagrams, see [Herrmann 2013].

3.1.3 Loading velocity

As presumed before, a variation of the loading velocity does neither result in a significant variation of results nor in a possible stabilisation of the numerical process. The graphs to prove the non- existence of influence cannot be shown here due to the brevity of the paper but also can be found in [Herrmann 2013].

3.2 Validation with additional comparisons

After the determination of the "best fitting" model A1msCDP2f70Psi45DP20 by comparing deflections and strains, this model shall be verified by further two dimensional examinations. Concrete crack patterns allow a fairly exact interpretation of the load bearing function and therefore are an excellent base of evaluation. Hence the test specimens were opened after the laboratory tests to uncover the cracked concrete cores.

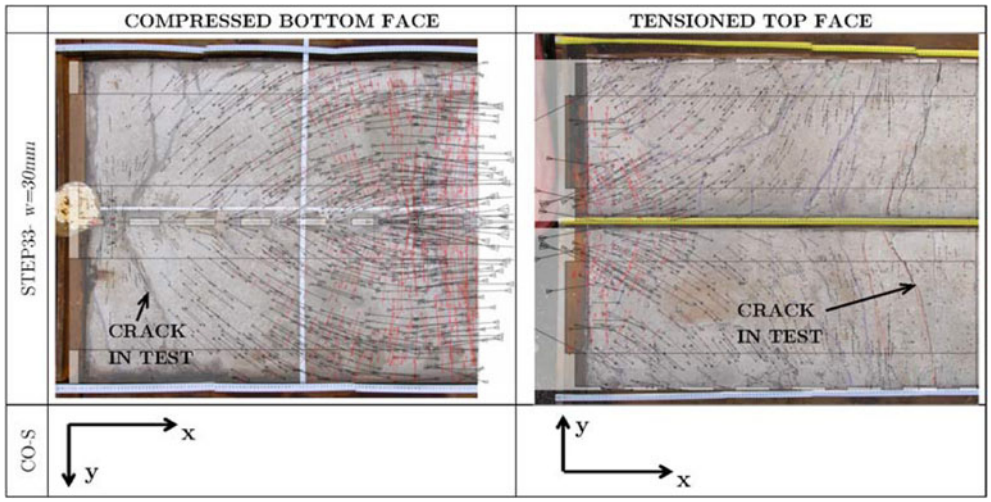

Figure 12: Concrete face crack patterns and trajectories of principal stresses

Fig 12 displays a comparison of the investigated crack patterns of the specimen's concrete faces after testing and the numerically determined trajectories of principal stresses. The black arrows thereby indicate the main compression and the red arrows the main tension stresses. As known, concrete parts always crack due to principal tension which is orthogonal to the principal compression direction per definition. This means that the trajectories of main compression can directly be compared to actual cracks. Both images, the compressed and the tensioned concrete face show excellent accordance of found cracks and theoretically determined principal stress directions.

Fig. 13 illustrates an overlay of actual cracks in the concrete core of the specimen after testing and the distribution of the stiffness degradation factors d_c and d_t. Coloured areas are areas of possible cracking. In red coloured areas the maximum decrease of d_t=0,99 is reached.

The correlation of physical cracks of the real structure and numerically investigated stiffness degradation is satisfying and the cracks are predicted in terms of position and intensity. Summing up, it is likely that the found FE-model is able to describe the effects within the SCSC-plate in an accurate way up to a load level of about 6000kN.

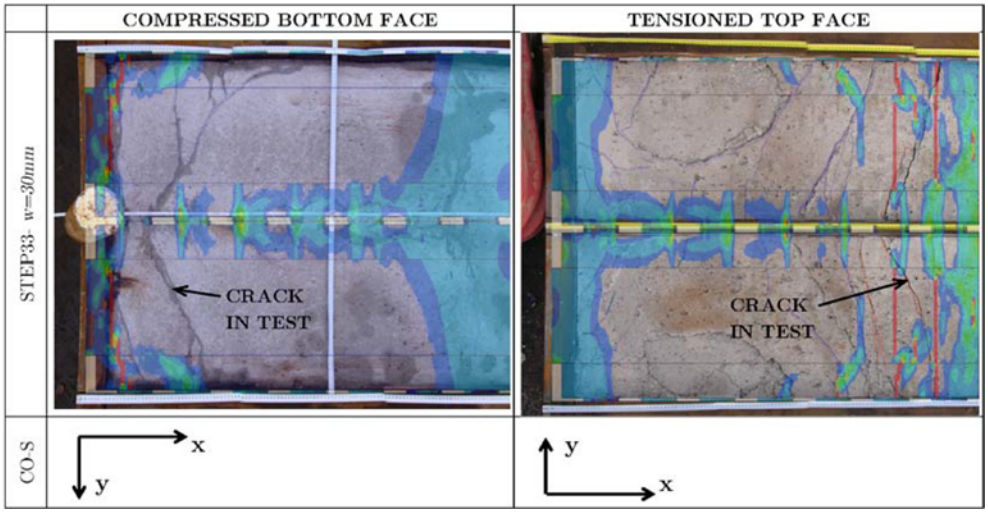

Figure 13: Concrete face crack patterns and distribution of stiffness degradation factors

4. Summary and outlook

The systematic investigation of the influence of non-measurable parameters of the concrete model CDP allowed identifying the "best- fitting" parameter combination to describe the structural behaviour of the test specimen by an FE- model. The goal to find an FE- model for the investigation of effects which are not measurable during laboratory tests can therefore be regarded as reached.

The next step is the derivation of further engineering models, using the obtained information of the numerical simulation. An applicable engineering model thereby needs to enable the design engineer to estimate the complex load bearing function of the SCSC- plate sufficiently accurate with a manageable investment of time and resources.

References

[Abaqus 2010a] Dassault Systemes: ABAQUS/CAE 6.10, 2010

[Abaqus 2010b] Dassault Systemes: Abaqus 6.10 Online Documentation, 2010

[Antesberger 2007] Antesberger, E.: Weiterführende numerische Untersuchungen zum Trag- und Verformungsverhalten von Kronendübeln. Masters Thesis, TU Vienna, 2007

[Fink et al. 2007] Fink, J.; Petraschek, T.; Ondris, L.: Push- Out Test Parametric Simulation Study of a New Sheet-Type Shear Connector. ZID- TU Vienna, 2007

[Fink et al. 2010] Fink, J.; Herrmann, P.; Juen, L.: Extremely slender steel and composite deck slab for railway bridges. IABSE Symposium, Venice, 2010

[Fink & Juen 2010] Fink, J.; Juen, L.: Innovative composite deck slab for railway bridges (1/2)- plastic strength behavior. 7th International Conference on Bridges across the Danube/ conference book, Sofia, 2010.

[Fink et al. 2011] Fink, J.; Herrmann, P.; Juen, L.: Extremely slender steel-concrete-composite deck slab for railway bridges - research, development, application. fib Symposium Prague, 2011

[Herrmann 2013] Herrmann, P.: Load bearing analysis and mathematical modelling for a new sandwich- composite plate (SCSC-Plate) as a deckslab for railway bridges. Doctoral Thesis, TU Vienna, 2013

[Juen & Fink 2011] Juen, L.; Fink, J.: Innovative composite deck slab for railway bridges - Technology, fabrication, laboratory tests and plastic load resistance estimation. Eurosteel 2011, Budapest, 2011

[Lee & Fenves 1998] Lee, J.; Fenves, G.: Plastic-Damage Model for Cyclic Loading of Concrete Structure. Journal of Engineering Mechanics, 1998

[Lubliner et al. 1989] Lubliner, J.; Oliver, J.; Oller, S., Onate, E.: A plastic-damage model for concrete, International Journal of Solids and Structures, 1989

[Zimmermann 2001] Zimmermann, S.: Finite Elemente und ihre Anwendung auf physikalisch und geometrisch nichtlineare Probleme. Technical University of Eindhoven, Netherlands, 2001